Stanford Exploration Project, Report 84, May 9, 2001, pages 1–255

4-D seismic monitoring of an active steamflood

David E. Lumley[1]

ABSTRACT

3-D migrations of time-lapse seismic monitor data acquired during steam injection show dramatic and complex changes in the reservoir zone over a wide area, compared to baseline seismic data recorded prior to steam injection. Anticipated large decreases in seismic P-wave velocity V_p near the injection well correlate with the presence of a hot desaturated steam zone. Unanticipated large *increases* in V_p in an annulus around the steam zone may correspond to a high-pressure cold oil front, in which residual free gas in pore space crosses the bubble point and dissolves into liquid oil. Horizontal and vertical anisotropy in flow directions inferred from these seismic observations correlate with two temperature monitor wells, and in situ measurements of upper and lower reservoir permeability. Since the pressure front propagates out from the injector an order of magnitude faster than either the thermal or steam fronts, monitoring it may be useful for predicting future fluid-flow paths of heated oil, months in advance of actual production.

INTRODUCTION

The steamflood process is a common method of enhanced oil recovery (EOR) in heavy oil reservoirs. However, steam flow directions, rates and sweep efficiency can be unpredictable in the presence of reservoir heterogeneity. This uncertainty can lead to expensive changes in injection well placement, intervals of perforation, and surface steam facility planning. Spatial changes in pressure, temperature and fluid saturation in the reservoir during steamflooding can cause dramatic changes in rock physics properties, and hence seismic wavefield attributes, e.g., Ito et al. (**?**), Wang and Nur (**?**). In principle, detecting and measuring changes in the seismic response as a function of time can lead to a better understanding of the steamflood fluid-flow dynamics, and in turn, can help optimize the production strategy for an EOR project (Nur, 1989). Although the concept of time-lapse seismic reservoir monitoring is relatively new, a few notable pilot projects have been attempted at EOR steam sites. Pullin et al. (1987) collected two 3-D seismic surveys before and after a steam pilot at an Athabasca tar sands reservoir site. By comparing time delay and amplitude attenuation maps between the two stacked surveys, they were able to qualitatively map the location of heated versus unheated zones. Their observed vertical traveltime delays and attenuations through heated sections of the reservoir compared reasonably well with rock physics studies of the predicted thermal ef-

[1]**email:** david@sep.stanford.edu

fects on seismic data. Eastwood et al. (**?**) performed a similar analysis on a 3-D seismic monitor of an Alberta cyclic steam stimulation (CSS) project. They used two 3-D seismic surveys recorded at separate production and injection cycles, integrated with crosswell data, thermal reservoir simulations, and rock physics measurements. They were able to fit the magnitude of changes between two surveys, but less so the spatial distribution of changes. Non-steam seismic monitoring projects of interest include an in-situ combustion study by Greaves and Fulp (1987), and a gascap monitoring study in the Oseberg field by Johnstad et al. (**?**). Currently, an ongoing 4-D seismic monitoring experiment is being conducted to monitor a steamflood in a shallow heavy oil reservoir in the Duri field, Indonesia. An excellent overview of the experiment and first interpretation of the field data has been presented by Bee et al. (**?**). Two baseline surveys were acquired before steam injection to demonstrate data repeatability. Five monitor surveys have been recorded so far at an average of 4 month intervals, ranging from 2 to 19 months after steam injection was initiated. Two temperature monitor wells are available, and six core samples were taken from the injector borehole pre-steam at various levels of the reservoir zone. I analyze this data set in collaboration with Bee et al. to understand the complex seismic changes observed between the repeated 3-D surveys in terms of changing reservoir parameters and fluid flow. In particular, I attempt to explain the complex seismic monitor phenomena by integrating a simple model of steamflood fluid-flow with rock physics measurements, finite-difference seismogram modeling, and 3-D prestack seismic imaging.

FIELD DESCRIPTION

Oil production

The 4-D seismic monitor data are recorded in the Duri Field, Indonesia. Bee et al. (**?**) review the field's history, current production, and describe the 4-D experiment and preliminary interpretation. The Duri Field contains 5.3 billion barrels (bbls) of original oil in place (OOIP). Primary production was expected to produce only about 400 million bbls, 8% of OOIP, because the Duri oils are very viscous (API gravity is 22 degrees). With steamflooding, about 60% of OOIP is expected to be recovered, representing an additional 2.7 billion bbls of oil over primary production. Currently, about 40% of the field is undergoing steamflooding. The first steamflood patterns were drilled in 1985 and have increased the field production from about 40,000 barrels per day (BPD) to currently over 285,000 BPD. Over $1.2 billion has been invested in steamflooding to date, and the project is expected to expand to completion for another 25 years. If seismic monitoring can increase production by only 1% of OOIP, an extra 53 million bbls of oil will be gained.

Reservoir quality

The main oil reservoirs are in very unconsolidated sands and silts at depth of 100–200 meters. Porosities and permeabilities are high and range from 30–38% and 1–8 darcies respectively. Oil saturation ranges from 29–69%, with a residual gas saturation of about 10% due to pressure drawdown during primary production. Duri oil is very heavy and viscous with an API

gravity of 22, and viscosities of 100–1000 cp. Clay layers can cause flow barriers, and heterogeneity can make steam flow directions unpredictable. For these reasons, a 4-D seismic monitor experiment was conducted on a small steam injection pattern to see if vertical and lateral steam flow could be mapped from seismic.

Steamflood pattern

Figure **??** shows a diagram of a single "7-spot" steam injection well pattern. The surface area of the 4-D seismic coverage is outlined by the outer box, and is 355 m on a side. The 7-spot is composed of six producing wells (black circles) connected in a hexagon, with the seventh well being the steam injector in the center (open circle with arrow). Additionally, two temperature observation wells (open circles) are located on either side of the injector.

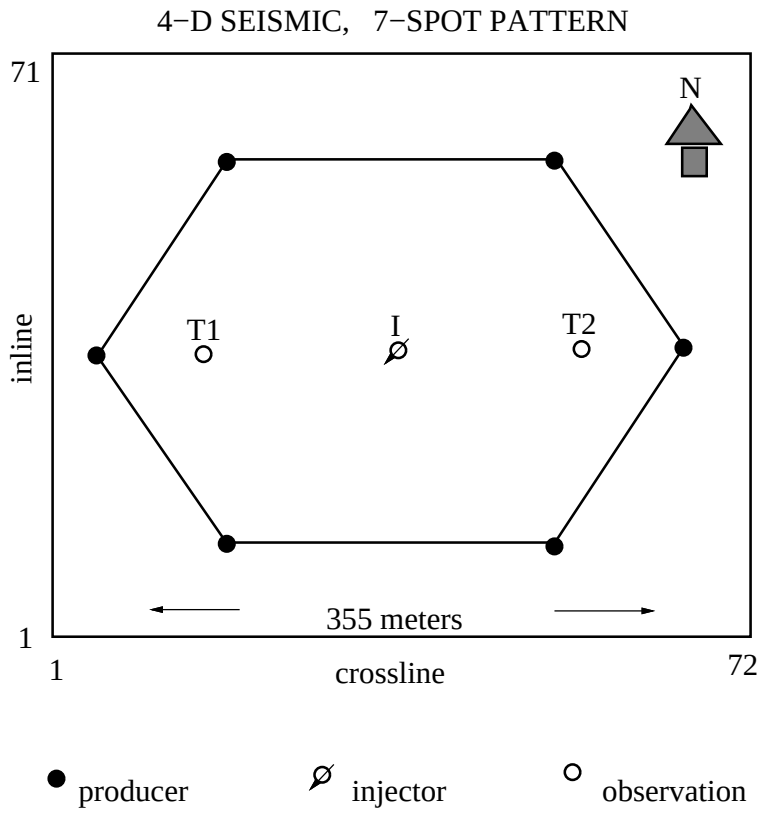

Figure 1: Duri 4-D seismic coverage over a single 7-spot production pattern. Steam injection well is at the center, flanked by two temperature monitor wells. david2-7-spot [NR]

4-D SEISMIC FIELD DATA

Seismic acquisition

Several 3-D seismic data sets have been acquired over the injector pattern of Figure **??**. Two baseline surveys were collected prior to steam injection for comparison with surveys taken during steam injection. The repeatability of the seismic measurements was confirmed with two baseline surveys to ensure that changes in repeated 3-D surveys were due to subsurface conditions, not acquisition-related variations. Each 3-D survey consists of 301 shots fired into a fixed array of 480 receivers. Each shotpoint consists of a small dynamite charge (50 g) fired in a shot hole at 45 ft. depth. Each receiver is a single hydrophone immersed in water at 20 ft. depth. Frequencies in the data exceed 200 Hz at a 1 ms sample interval. The maximum offset in the data is 480 m, with a good range of offset and azimuthal coverage. Maximum fold is 80 in the center of the pattern. A complete 3-D survey can be acquired in one day. Figure **??** shows the bin centers for the 3-D survey, and Figure **??** shows the fold chart. To date, five repeated seismic monitor surveys have been obtained with identical acquisition parameters. Shot and receiver holes were predrilled and reoccupied for each monitor survey. Both sets of holes are cased down to just above the source or shot depth. Dynamite charges were lowered and tamped with sand for each survey, and the small charge size was chosen for good bandwidth and negligible hole damage. Hydrophones were lowered into each receiver hole and filled with water. Repeat surveys were acquired at intervals ranging from two months after steam injection, to 19 months after steam injection, with an average 4 month repeat interval. In this paper, I will concentrate on the baseline survey and the second monitor after 5 months of steam injection.

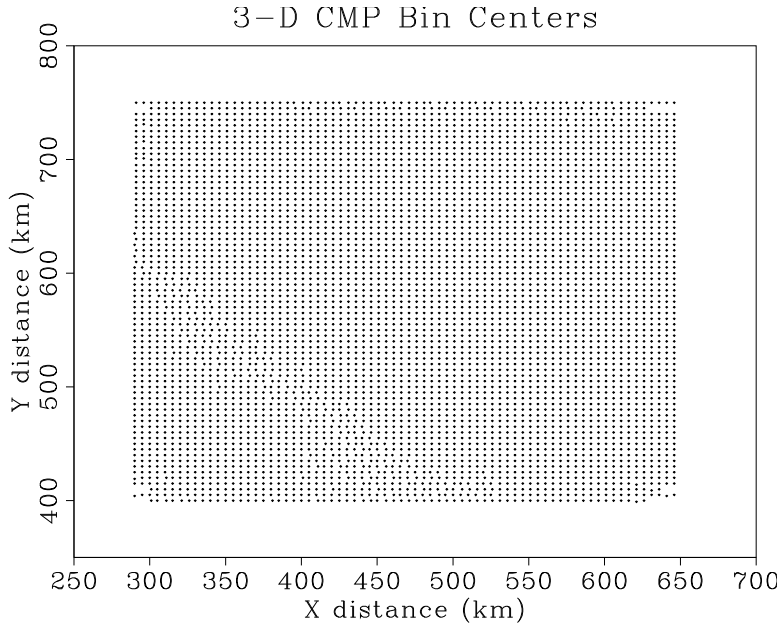

Figure 2: 3-D survey CMP bin center locations. Seismic “inlines” are horizontal, “crosslines” are vertical. david2-cmpbins [ER]

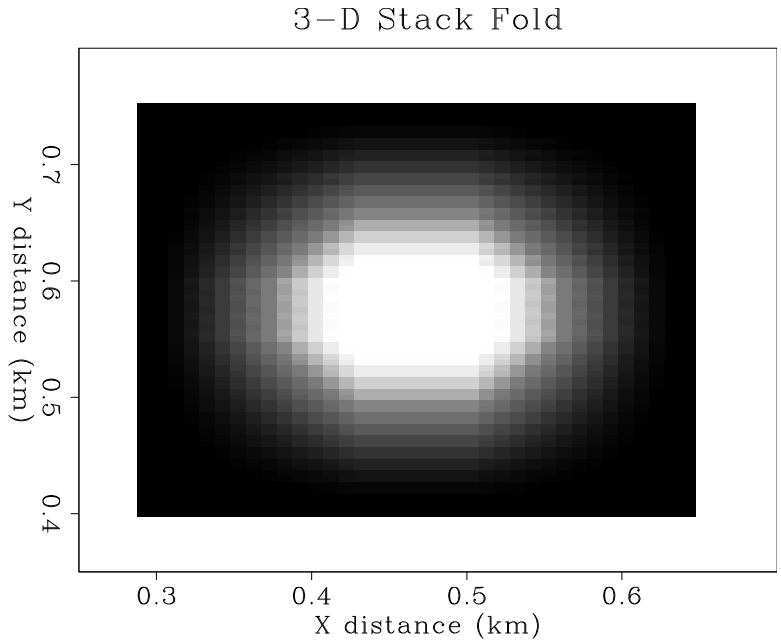

Figure 3: 3-D survey stack fold. The fold is about 2 at the survey edges, and a maximum of 80 in the center white patch. david2-stkfold [ER]

Field data

Figure **??** shows 3-D stacked inline sections of the baseline, monitor and the difference between the two. The location of the inline sections passes through the two temperature observation wells and the steam injector. Figure **??** shows the same display of 3-D migrated inline data. Figure **??** shows a time slice at 204 ms before and after steam injection. The top of the main reservoir is at about 160 ms, and the base is just below 200 ms. Steam had been injected continuously into this zone for five months at the time of this monitor survey. The inline stacks and migrations show that data above the reservoir (less than 150 ms) is highly repeatable. The only major difference above the reservoir is the effect of the borehole region being heated by a possible steam leak causing time sag in the center of the profile. This is most notable in the migrated section of Figure **??**, and labeled with a "B". The stacked sections show a large diffraction response, labeled "D", which has an apex at about 200 ms, at the base of the reservoir. Weaker diffraction responses are less visible at the top of the reservoir around 160 ms. These diffractions are probably due to the steam zone, as will be demonstrated in the seismic modeling section of this paper. The migrated sections in Figure **??** show that major changes in the seismic data have occurred near the injection well (center) within the reservoir zone from 160–200 ms. The bright reflections labeled "S" are probably due to presence of steam, and cause time sag (velocity decrease) below the reservoir at the injector site. A very anomalous polarity change has been caused by the process of steamflooding, and is labeled "P" in the sections. This strong polarity change is visible in both the stacked and migrated sections, and is asymmetric in that it occurs on one side of the injector, but not the other. Additionally, there appear to be some time pull-ups (velocity increase) very close to the injector, which give a si-

nusoidal shape to the reflector at 200 ms, most visible in the monitor migration. The difference sections show that within the reservoir zone only a narrow width of about 50 m is affected by steam injection. However, below the reservoir base of 200 ms, large changes have occurred in the seismic data for a full 350 m out to both edges of the survey. The time slices at 204 ms in Figure **??** show dramatic change at the base of the reservoir. A bright reflective disk with a diameter of 50 m, labeled "S", is centered about the injector, surrounded by a thin (20 m) dark gray annulus. A larger black "front" extends out to the edge of the survey to the east and south, labeled "P", and corresponds to the polarity reversal seen in the inline sections.

Questions

Since reflections from the region above the top of the reservoir are seen to be very repeatable in both surveys, we can be certain that changes in and below the reservoir are due to the steamflood process. These dramatic changes in seismic data during 5 months of steam injection raise many interesting questions.

- Do the bright reflections and time sag in the reservoir indicate the presence of steam, or merely hot fluid?
- Should we be able to distinguish separate fluid-fronts of water, oil and steam?
- What could be causing time pull-up (velocity increase?) near the injector?
- What is the explanation for the large polarity reversal along the base of reservoir reflection, and its asymmetry?
- Why are changes within the reservoir confined to a width of only 50 m, whereas changes below the reservoir extend at least 350 m out to the edge of the survey area?

In the following sections, I attempt to answer some of these questions by carefully considering steamflood fluid-flow physics, rock physics measurements, and finite-difference seismic modeling in comparison with these data displays.

RESERVOIR FLUID FLOW

Reservoir conditions

The seismic monitor data were recorded over a 7-spot steamflood pattern (six producing wells in a hexagon plus one central injector), and fits within a square of about 350 m on a side. The main reservoir zone is at approximately 200 m depth and consists of very unconsolidated sands, silts and clays. Porosity and permeability range from 37–42% and 1.2–8.5 Darcy respectively. The heavy oil has an API gravity of 22 degrees, and viscosities of 150–1000 cp. Oil saturations range from 29–69%, and there is a residual gas saturation of about 10% in pore space caused by previous pressure depletion. The overburden pressure is 530 psi, and

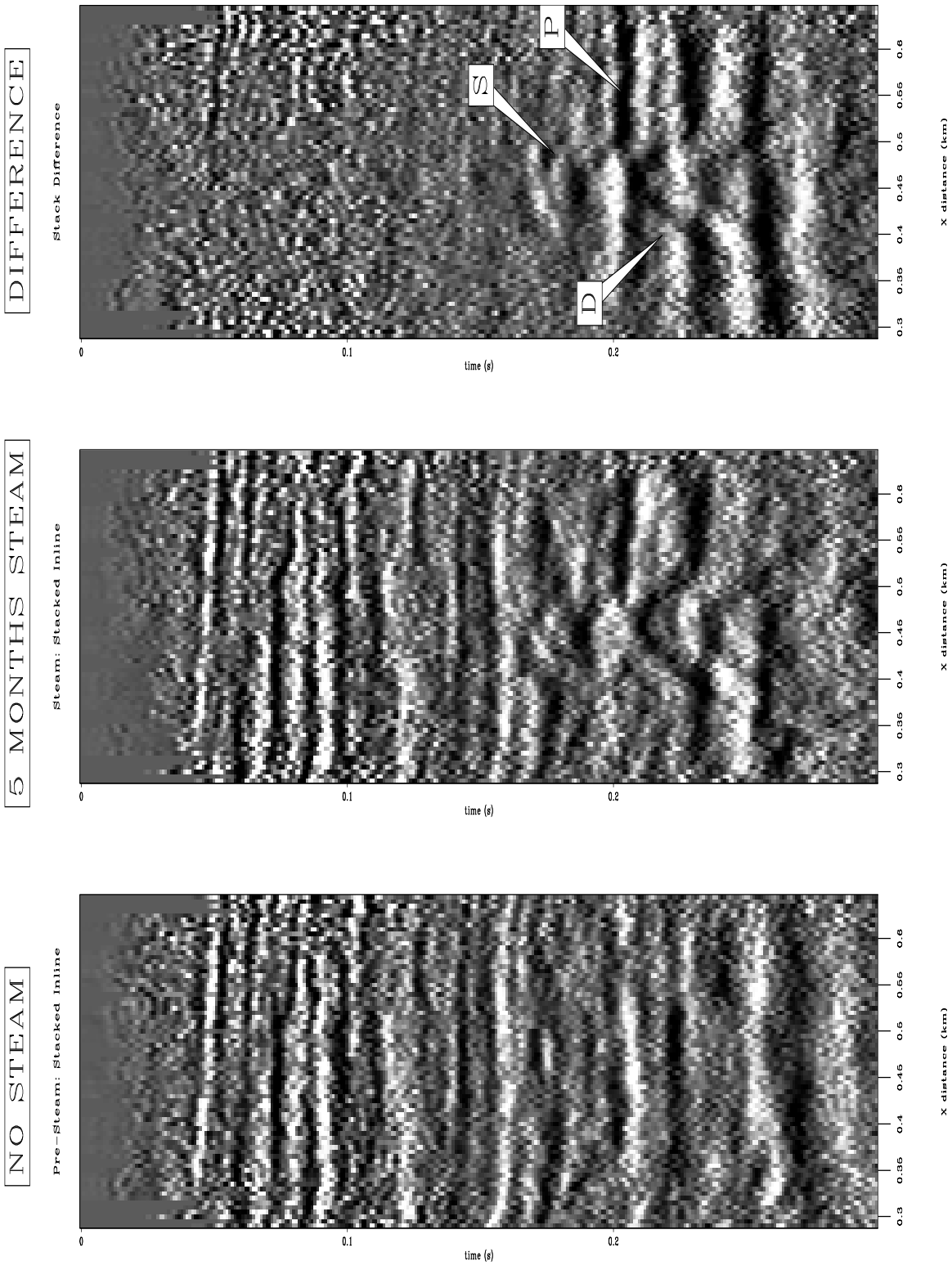

Figure 4: 3-D stacked inline sections: before steam injection (left), during steam (center), and the difference (right). "S" marks a steam zone, "D" marks a diffraction, and "P" marks a polarity reversal. david2-inline-stks-ann [ER,M]

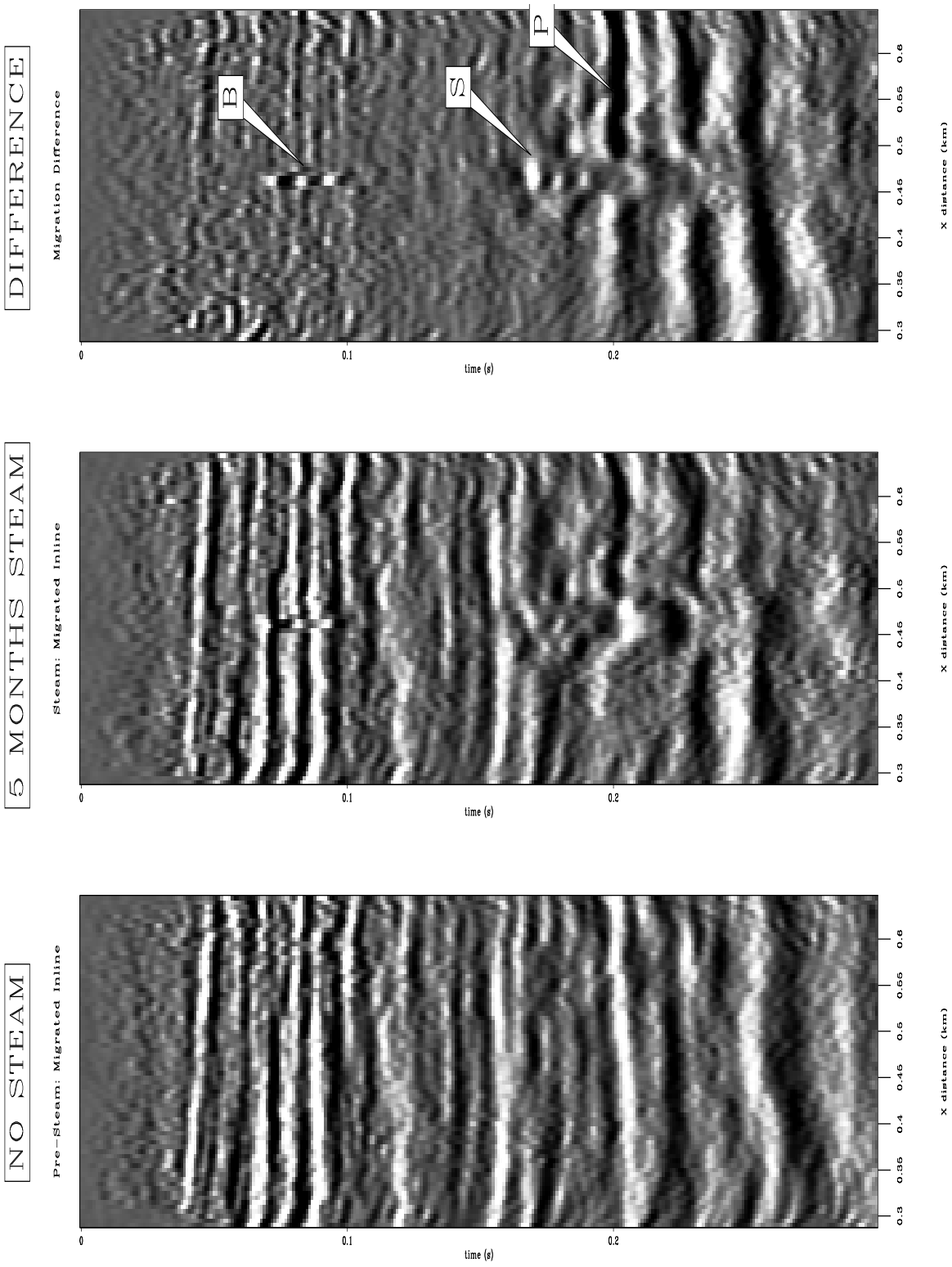

Figure 5: 3-D migrated inline sections: before steam injection (left), during steam (center), and the difference (right). “S” marks a steam zone, “B” marks borehole heating by a possible steam leak, and “P” marks a polarity reversal. david2-inline-migs-ann [ER,M]

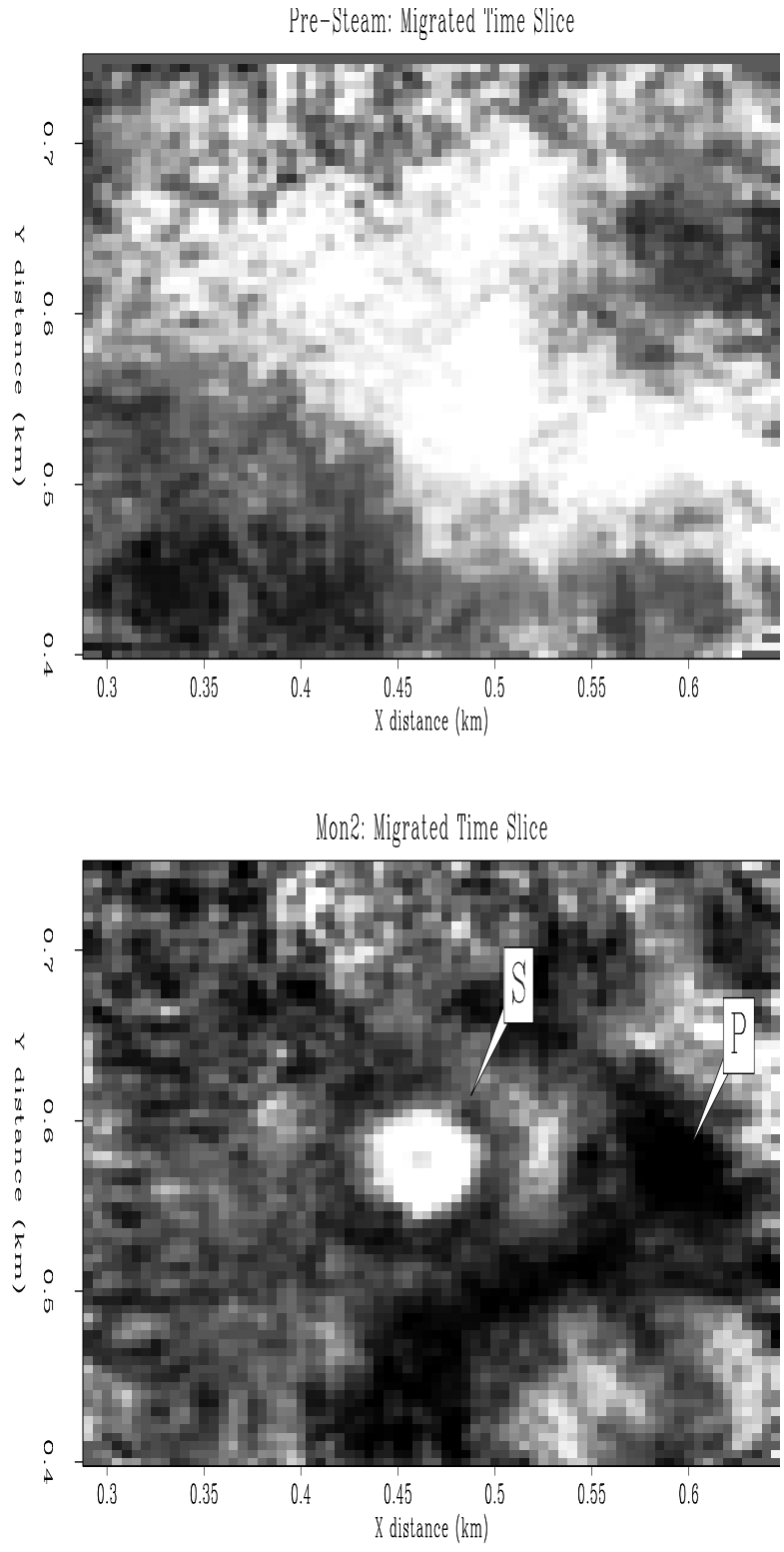

Figure 6: 3-D migrated time slices at the base of the reservoir (204 ms): before steam injection (top), and after 5 months of steam injection (bottom). "S" marks the steam zone, and "P" marks the polarity reversal associated with a possible high-pressure front. david2-tslice-migs-ann [ER]

pore pressures range from 100 psi (pre-steam) to 350 psi at the injector during steamflooding. Reservoir temperatures range from 100 F (ambient) to 350 F (steam).

Steamflood model

It is convenient to have an idealized model of the steamflood fluid-flow physical properties in order to make some predictions about the nature of rock physics and seismic responses during steam injection. I consider four separate fluid zones associated with the steamflood: (1) a high-pressure, low-temperature heavy oil zone, (2) a high-pressure, high-temperature heavy oil zone, (3) a high-pressure, high-temperature water zone, and (4) a high-pressure, high-temperature desaturated steam zone. This simple model is schematically diagrammed in Figure **??**. This model is slightly more complicated than the conventional block model of a heated zone and a cold zone, but does not try to incorporate the complexity of mixed fluid phases, emulsions, fingering, gravity overrides, etc., as described by Lake (**?**) for example.

This model is qualitatively supported by common observations. In well-to-well pressure transient tests, it takes on the order of hours to days for a pressure pulse at one well to propagate to an adjacent well. Pressure is transmitted through the fluid in the connected pore space at a relatively fast rate because it does not require fluid transport or conduction to diffusively propagate. On the other hand, temperature monitoring wells show that thermal fronts take on the order of weeks to months to propagate similar well-to-well distances. This is because heat transfer must occur through a combination of conduction through the rock matrix and convective transport of heated fluids through the permeable pore space, both of which tend to be relatively slow processes. A desaturated steam front propagates even slower than a thermal front, because of the additional work required to drive fluids out of pore space. Therefore, to first approximation, a steam-induced pressure front will travel about one order of magnitude faster than the associated thermal front. This implies that to a distant observer in the reservoir, the first front to arrive will be a high-pressure cold oil front. The next zone to arrive will be high-pressure heated oil as the thermal effects propagate outward from the steam injector. A hot water zone of condensed steam follows and heats the oil ahead of it, lowering the oil viscosity enough to displace oil with water as it propagates radially away from the injector. Finally, closest to the injector, a hot steam zone with negligible fluid saturation exists as the heat source that drives the total fluid-flow process. It is likely that the steam zone would reach steady-state equilibrium conditions fairly quickly and maintain a stable but slowly expanding disk of growth. In contrast, the pressure front is likely to be large and may propagate rapidly to remote sections of the reservoir. The hot oil and water zones are probably intermediate in size between the steam and high-pressure cold zones.

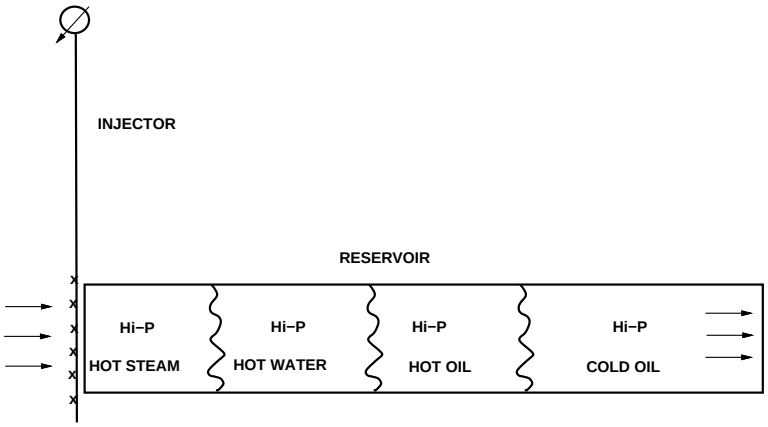

Figure 7: An idealized model of steamflood fluid flow. A rapid high-pressure cold front is expected to lead the injector flow, trailed by hot oil, hot water and hot steam zones. The relative dimensions of each zone may not be to scale, and complexities such as mixed phases and gravity overrides are neglected. david2-steam-fronts [NR]

ROCK PHYSICS

Core measurements

Rock physics core measurements were made by Zhijing Wang at Chevron's research facility. Six core samples were taken from the injection well location prior to steamflooding. The samples range from clean fine sand, to clay/silt/sand. The samples show highly unconsolidated sedimentary material. Some samples show coarse sand pockets which might represent potential high-porosity, high-permeability micro channels. The core samples were found to be very sensitive to pressure and temperature conditions. V_p decreases of 10–19% were measured for temperature increases from 25 C to 177 C at fixed overburden pressure (530 psi) for core samples saturated with 30–70% oil. An additional V_p decrease of 12–28% for the same temperature increase was measured on samples in which fluid had been replaced with steam (gas). At fixed overburden pressure and temperature, V_p decreases 3–9% as pore pressure increases from 100 psi to 400 psi in saturated samples. This is due to grain matrix compaction alone, not any phase change in the pore fluid. The effect of a decrease in gas saturation from 10% to 0% results in a velocity increase of 19–26%. An increase in gas saturation from 10% to 25% or more results in a 10–15% decrease in velocity.

Steamflood properties

Based on the simple steamflood model of Figure **??**, and the core measurement data at Duri, some rock physics analysis can be made to give approximate estimates of seismic velocity changes that may occur in the reservoir during the steamflood. These rock physics predictions give an indication as to what might be observed in time-lapse 3-D surface seismic monitor

surveys. The effects of pressure, temperature, gas/fluid saturation, and hydrocarbon P-T phase diagrams are considered for each of the four steamflood fluid-flow zones described previously.

Hi-pressure cold oil front

As the Duri core measurements show, P-wave velocity V_p varies with differential pressure, which is the difference between overburden and pore pressure. Overburden pressure is about 530 psi in the main Duri reservoir. Ambient pore pressure before steam injection is about 100 psi due to depressurization during primary production. During steam injection, the pore pressure at the injector may be as high as 350 psi, and would decay logarithmically with radial distance from the injector. This pore pressure increase of 200-300 psi due to steam injection decreases the P-wave velocity by about 3–9% depending on the matrix consolidation of the core sample. Additionally, the Duri reservoir is initially below bubble point, since there is residual gas saturation of about 10%. The bubble point is defined as the contour in P-T phase space where decreasing the pressure at fixed temperature will cause 100% liquid oil to begin forming gas bubbles, as shown in Figure **??**. Duri engineers estimate that an increase of only 10 psi at 100 F is sufficient to dissolve the free gas back into liquid phase. Therefore, the initial 10% free gas in the reservoir is dissolved back into liquid oil as the high-pressure front propagates. This situation is depicted by the path A–B in the hydrocarbon phase diagram of Figure **??**: an increase in pressure at fixed temperature crosses the bubble point line (**?**). The change from an oil saturation of 0.9 to 1.0 can cause a dramatic increase in V_p, as first described by Domenico (**?**). Figure **??** shows Domenico's experimental results that V_p can increase by at least 10% in this regime of fluid saturation contrast. Duri core measurements show that saturated samples increase in velocity by about 26% at 200 psi pore pressure. The larger change compared to Domenico's results is probably attributed to the highly unconsolidated nature of Duri reservoir sands. Combining the effects of pore pressure increase and gas saturation decrease across the bubble point, a net velocity increase of at least 17–23% is expected in the high-pressure cold oil front compared to initial reservoir conditions, as shown in Figure **??**.

Hot oil zone

Wang and Nur (**?**) performed experiments which showed the effects of temperature and oil/water/gas saturation on Ottawa sandstone, as diagrammed in Figure **??**. Assuming hot oil displaces original cold oil, Figure **??** shows that this effect can cause V_p to decrease by about 15%. This compares well with Duri measurements of velocity decreases on the order of 10–19% for a 150 C temperature increase. This accompanies a velocity decrease of 3–9% for a pore pressure increase which softens the pores. However, when both pressure and temperature increase, the gas saturation level may also change. To predict the latter, the bubble point pressure needs to be known for the reservoir oil as a function of temperature, which is the uppermost contour in Figure **??**. Without knowing the exact shape of the phase space, an increase in both P and T can lead to total gas dissolution (path A–C), or can result in an increase in gas saturation (path A–D). Normally, one would expect the bubble point to increase

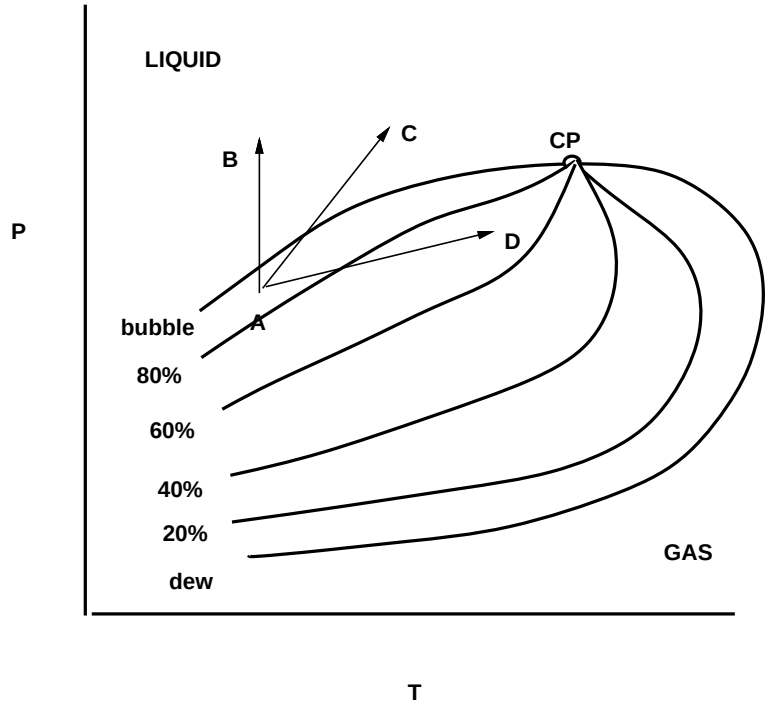

Figure 8: Hydrocarbon phase diagram with contours of liquid oil saturation relative to gas. CP is the critical point, P-T is the pressure-temperature plane (after Dake, 1978). david2-hc-phase [NR]

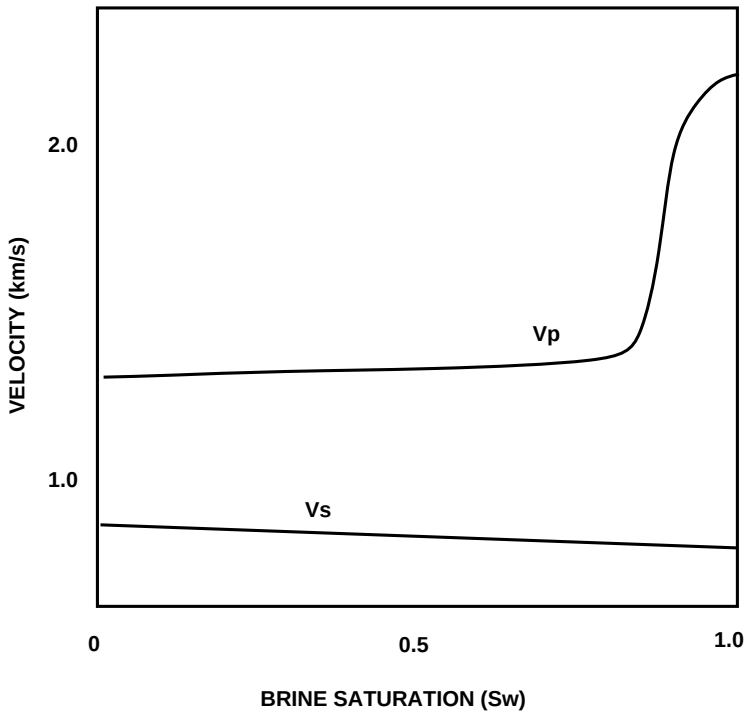

Figure 9: V_p and V_s versus brine saturation for Ottawa sandstone at a differential pressure of 10 MPa (after Domenico, 1977). david2-vp-sat [NR]

slowly with temperature, such that a large pore pressure increase from 100 psi to 300 psi at hot oil temperatures of about 100 C would reduce the gas saturation, or totally dissolve it (path A–C). This would again increase the velocity by about 22% at 200 psi pore pressure due to the Domenico effect as shown Figure **??**. The net effect of temperature increase, pore pressure increase and some reduction in gas saturation might make a net velocity change of about -6% to +9% in the hot oil zone, as shown in Figure **??**. These values suggest that the oil zone could be accompanied by either a small velocity increase or decrease, and therefore might be seismically transparent.

Hot water zone

The hot water zone should have a simpler physical behavior compared to the case of hot/cold high-pressure oil at or near the bubble point. In this case, both hot oil and any residual gas saturation is largely driven out by a hot water bank. The V_p contrast should be similar to moving from the cold oil curve to the hot water curve in Figure **??**, which suggest a small velocity decrease of about 5%. This accompanies the velocity decrease of 3–9% due to pore pressure increase softening the pores. Adding in the effect of decreased gas saturation causing a 22% increase in velocity, a net velocity increase of about 10–16% is expected in the hot water zone, as shown in Figure **??**.

Steam zone

When the steam zone arrives, nearly all fluid is driven out of the pore space, and is the primary mechanism for driving the hot water zone forward. Figure **??** shows that the change from initial cold oil to hot steam causes a dramatic decrease in V_p by about 30%. Note that about 25% of this decrease is due to the gas saturation change effect, and only a a further decrease of 5% is added by the thermal effect. The Duri core measurements show that the increased temperature causes a 10% decrease in velocity. The gas saturation increase from an initial 10% to greater than 25% causes a further velocity decrease of 10%. The pore pressure increase causes an additional 3–9% decrease in velocity. The net effect is an approximate 23–30% velocity decrease in the steamed zone, as shown in Figure **??**.

Velocity contrast profile

Figure **??** shows the predicted velocity contrast profile in the radial direction away from the injector, obtained by combining the rock physics results above. An impedance profile should look similar since density changes will be approximately the same polarity as velocity changes within each front. The rapidly outward-propagating pressure front leads the thermal fronts, and if the reservoir is initially just below the bubble point pressure, the pressure front will appear seismically as an increase in V_p by about 20%, marked by velocity time pull-ups and a positive reflection coefficient. The thermal fronts are likely to lag behind the leading pressure front by many months of steam injection. The outermost thermal front is likely to contain hot

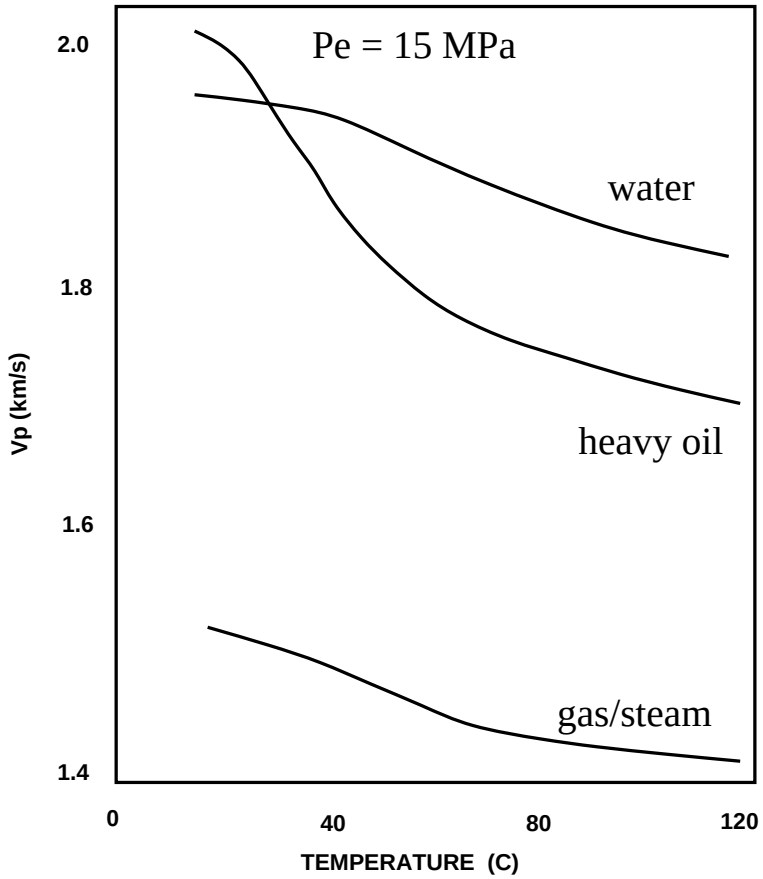

Figure 10: V_p measurements as a function of temperature and saturation with air, water and heavy crude in Ottawa sandstone (after Wang and Nur, 1988). david2-vp-temp [NR]

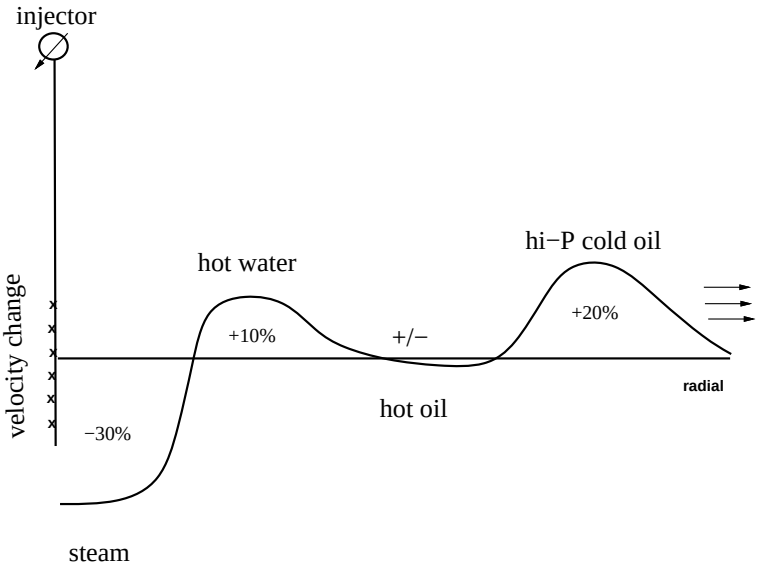

Figure 11: Predicted steamflood P-wave velocity changes compared to initial reservoir conditions as a function of dimensionless radial distance. david2-steam-dIp [NR]

oil and be nearly seismically transparent, since it can have either a small velocity increase or decrease of about 6–9%. Just behind the hot oil front, a hot water front may exist. It represents a velocity increase of 10–16% if the initial 10% gas saturation is driven away. Finally, a small stable steam zone should surround the injector, perhaps growing in diameter at a very slow rate. This steam zone has a net decrease in V_p of about 23–30% and should be very visible in the seismic monitor data by strong velocity pull-down and very bright negative reflection coefficient polarity.

SEISMIC MODELING

Combining the steamflood model and rock physics analysis, I now show some finite-difference seismogram modeling to examine what the seismic response to steamflooding might look like. I show simple velocity models of the steamflood, wavefield snapshots, shot gathers, and plane-wave stacks.

Velocity models

Figure **??** shows three 1-D velocity profiles. Each one is identical except for the reservoir zone containing either: original cold oil, steam, or the high-pressure front. The velocity model before steam injection is shown in Figure **??**, and after steam injection in Figure **??**. Note that after steam injection there is a large low velocity zone near the injector, and a high-velocity high-pressure front propagating in an annulus away from the injector.

Point-source modeling

Using the velocity models of Figures **??** and **??**, I simulated shot gathers by finite difference acoustic modeling. The shot is located at the injector location, and the data are modeled with about 200 Hz maximum frequency content, to match the field data. Figure **??** shows a snapshot of the wavefield before and after steam injection. Note that the steam snapshot has a much larger upgoing reflection branch, and is slightly flattened due to time delay on the leading downgoing branch. Figure **??** shows the shot gathers corresponding to the two point-source shots before and after steam injection. Note that the top of reservoir reflection at 210 ms has changed dramatically. It is much brighter and contains a polarity reversal. This polarity reversal occurs where the low-velocity steam zone transitions into the high-velocity pressure front. This polarity effect might explain the polarity reversal seen in the field data of Figures **??** and **??**, and suggest that there is a pressure front in the field data. Finally, note the diffractions from the steam zone. These also match diffractions seen in the field data, and suggest the lateral extent of a steam zone.

Plane-wave modeling

Figure **??** shows a finite difference acoustic simulation of a plane wave source leaving the surface at vertical incidence. The snapshot shows that the plane-wave is delayed by the steam zone in the center at the injection well, compared to the pre-steam synthetic. Diffractions are clearly visible at the center point. The outer limbs of the plane wave are pulled up in time, but the effect is too small to see in a static display. Figure **??** shows the "wave-stack", Schultz and Claerbout (**?**), that would have been recorded at the surface for the vertically incident plane-wave source. This wave-stack is similar to an NMO stack section, except it makes no velocity assumption. Note the presence of a strong diffraction associated with the steam zone. Also note the polarity changes and zero crossing along the top reservoir reflection from the steam zone to the high-pressure zone. The wave-stack clearly shows velocity time sag and amplitude focusing below the steam zone, and time pull-up at the survey edges beneath the portion of the reservoir containing the high-pressure front. All of these effects are somewhat visible in the field data sections of Figures **??** and **??**.

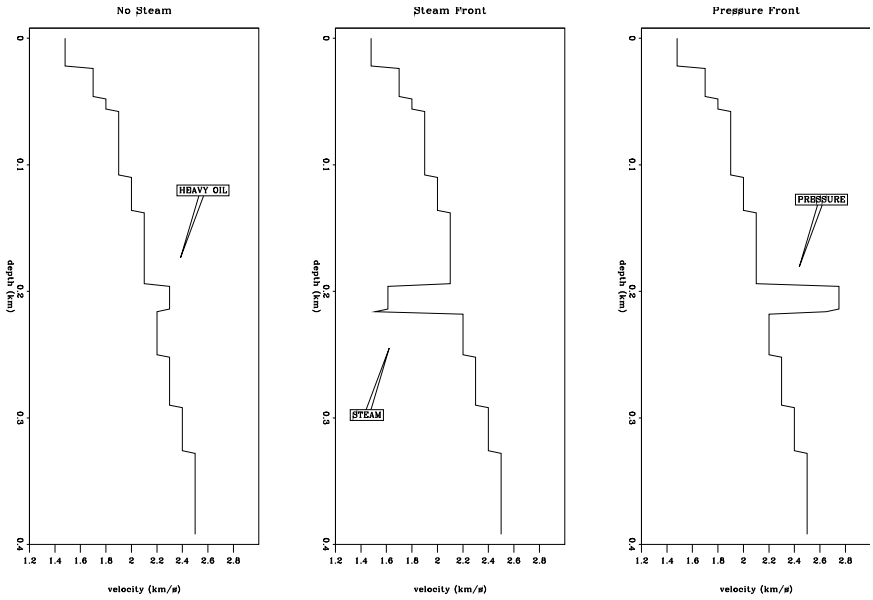

Figure 12: Velocity profiles of reservoir containing: heavy oil (left), steam (center), and high-pressure dissolved gas (right). david2-vp123g-ann [ER]

DISCUSSION

In this section, I interpret the combined analysis of the steamflood model, rock physics, seismic modeling, and field data observations. It appears that the bright reflection disk centered on the injector well and the time sag beneath must indicate the extent of the steam zone, not merely hot fluid. The rock physics analysis has shown that the steam zone should be expected to show velocity decreases of up to 30%, whereas hot water or oil increases velocity by only

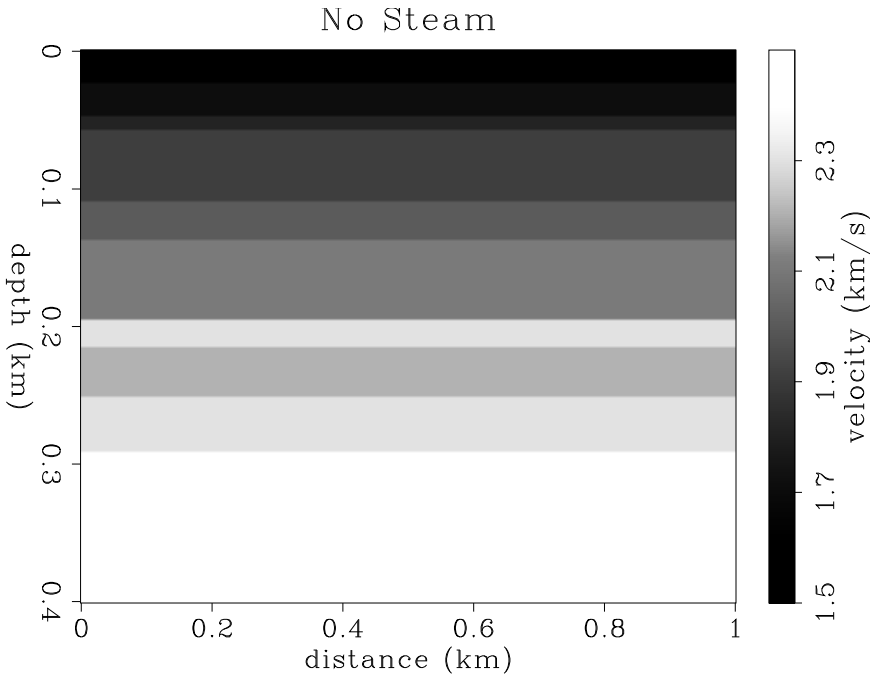

Figure 13: Velocity model before steam injection. Heavy-oil reservoir is at 200 m depth. david2-vp1 [ER]

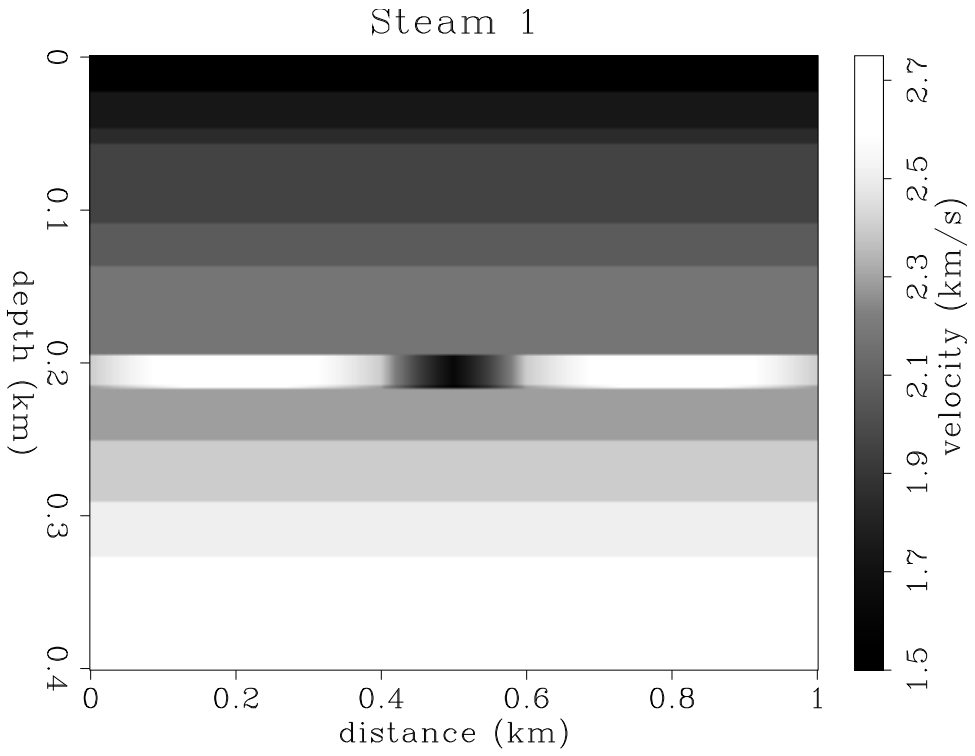

Figure 14: Velocity model after 5 months of steam injection. Low velocity anomaly in the center (dark gray) is due to steam, high velocity anomalies on the flanks (white) are due to the high-pressure front. david2-vp2 [ER]

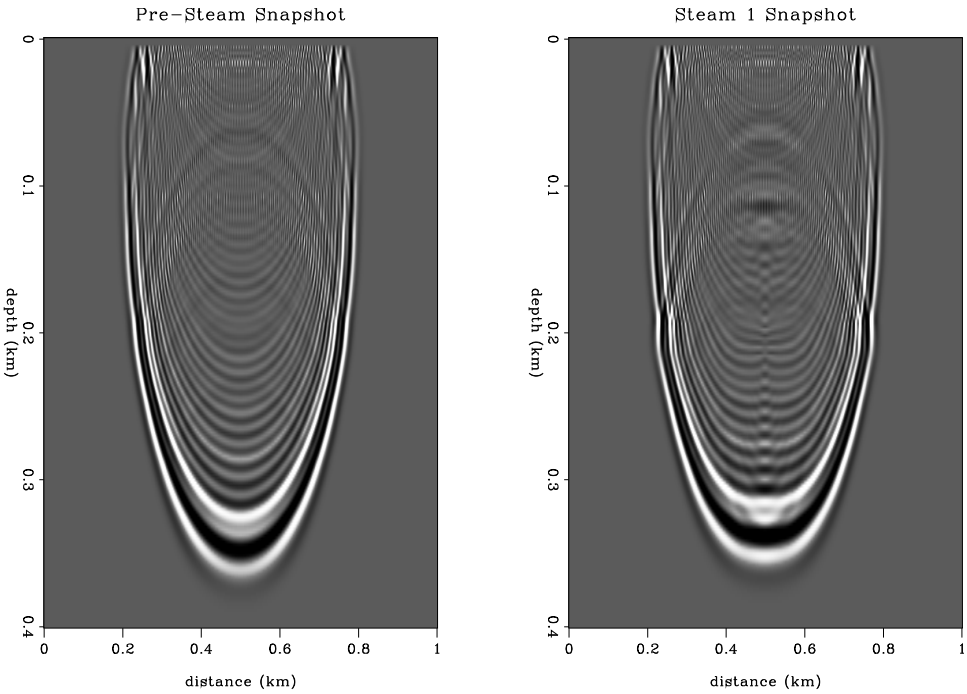

Figure 15: FD acoustic modeling wavefield snapshots: before steam injection (left), during steam (right). david2-waves12 [ER]

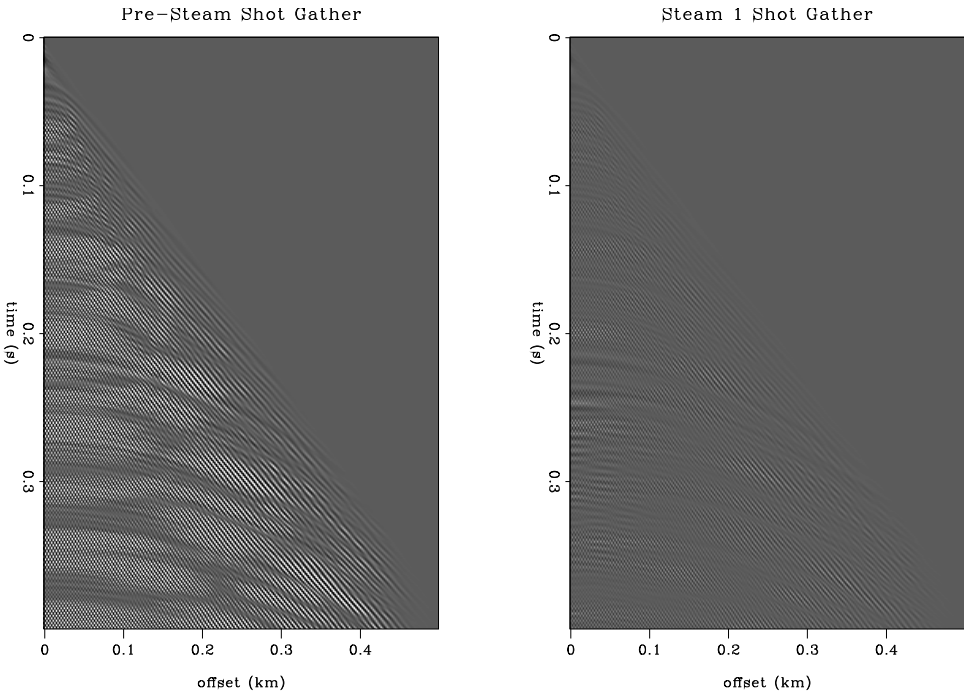

Figure 16: FD acoustic modeled shot gathers: before steam injection (left), during steam (right). david2-shot12 [ER]

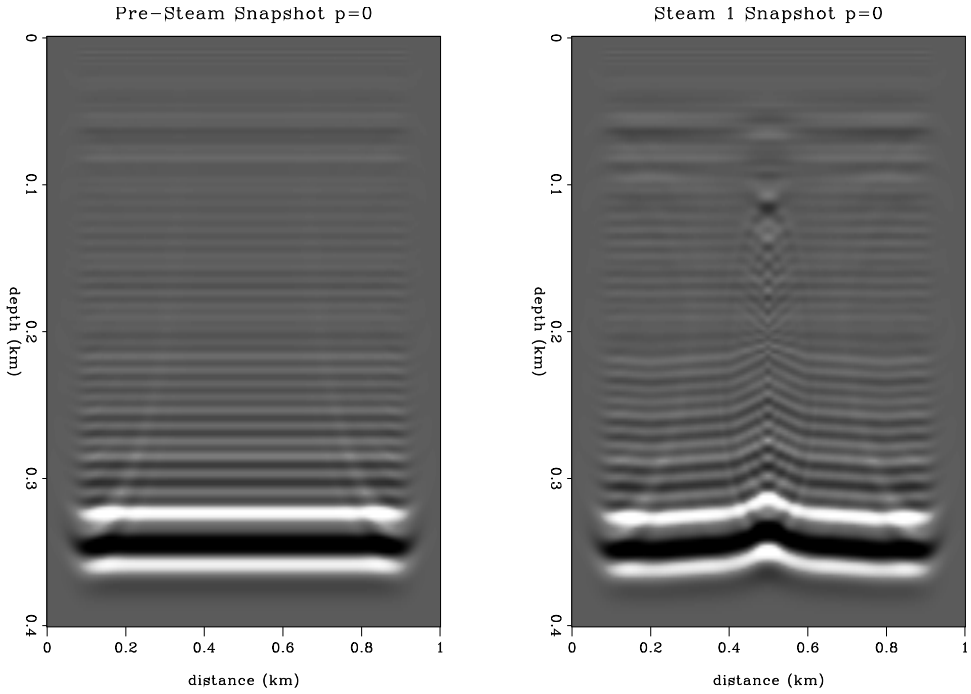

Figure 17: FD acoustic planewave snapshots (p=0): before steam injection (left), during steam (right). david2-pwave12 [ER]

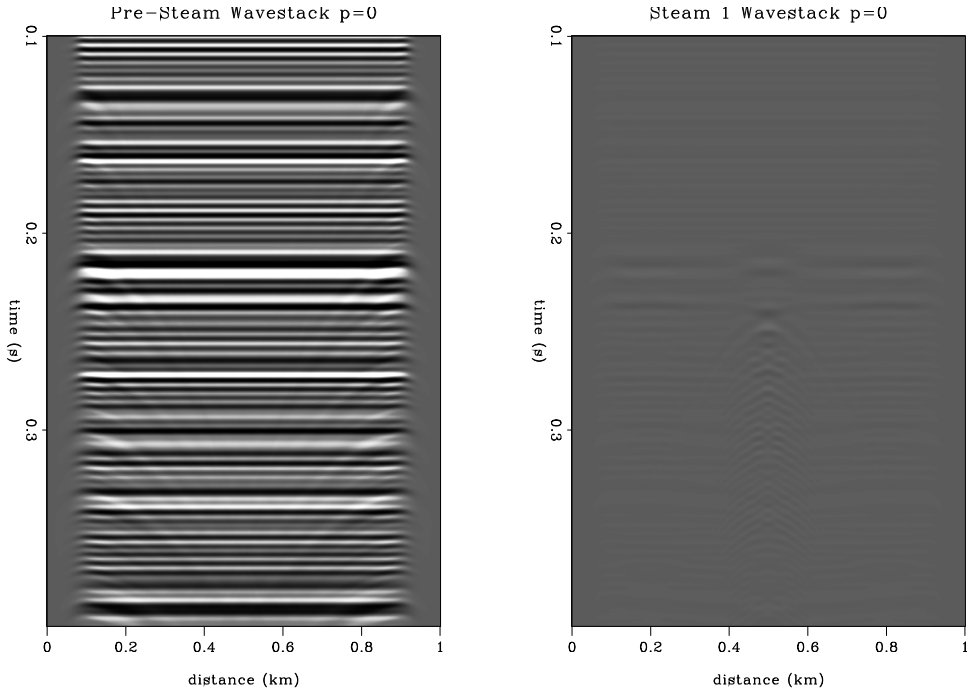

Figure 18: FD acoustic planewave wavestacks (p=0): before steam injection (left), during steam (right). david2-wstk12 [ER]

10% or less. Finite difference modeling of a reasonable steamflood velocity model shows strong diffractions and bright reflections emanating from the steam zone, that can be interpreted to match similar features in the field data. This analysis implies that the steam zone is about 25 m in diameter at the top of the reservoir, 50 m in diameter at the base of the reservoir, and possibly heading west faster than east. This correlates with core measurements that the top part of the reservoir is at least one order of magnitude less permeable than the bottom part, and that at 5 months of steam injection, substantial heating has arrived at the T1 temperature monitor well to the west, but not the T2 well to the east. My analysis suggests that the hot oil ring may be seismically transparent, but that the hot water ring might be visible since it causes a 10–15% velocity increase. Close inspection of the time slice in Figure **??** shows a thin dark gray ring surrounding the white steam disk. This ring is about 25 m thick and corresponds to time pull-up (velocity increase) in the migrated inline section of Figure **??**. The dark gray amplitude suggests it is opposite reflection polarity to the steam zone, which matches the predicted hot water properties. Perhaps this dark gray ring is the seismic view of the hot water annulus. I predict that a large area of the 7-spot pattern should be subject to a fast-propagating high-pressure cold oil front. This pressure front should be seismically visible since it causes a 20% increase in velocity. Finite difference modeling shows that the high-pressure front can cause polarity reversals on seismic events and time pull-up due to velocity increase. Figures **??** and **??** show these polarity effects to the south and east of the injector, which are in the opposite direction to the fastest heat propagation direction given by the temperature observation wells. Perhaps the pressure front has already propagated past the edge of the survey to the north-west, but is moving slower, and thus still visible, to the south-east. Below the reservoir base of 200 ms, large seismic changes occur all the way to the edge of the 7-spot pattern. This could coincide with the fact that the pressure front has travelled quickly to the edges of the pattern, and effects only those reflectors below the base of the reservoir, not within or above. These seismic changes below the reservoir base could be caused by time pull-up due to the pressure front velocity increase. The dark gray reflectivity of a large outer semi-ring might be interpreted as the pressure front in Figure **??**.

ONGOING WORK

I continue to work with this complex and fascinating data set. I am working with all five 3-D seismic monitor data sets, and incorporating well log information. I am also working to properly 3-D depth migrate these data after depth migration velocity analysis. I may use experience in 3-D AVO analysis to sort out velocity versus reflectivity changes in this data, if necessary. I hope to better understand the seismic changes from survey to survey, and test whether the pressure front can be used as a tool to predict future thermal fluid flow months in advance.

CONCLUSIONS

I have attempted to explain changes in seismic monitoring data sets acquired over an active steamflood project. By combining field data observations with a steamflood fluid-flow model, rock physics analysis and seismic modeling, I have assembled a plausible interpretation of the field data. A disk of steam can be seen in the seismic data that extends to a diameter of about 50 m, surrounded by what may be a 20 m annulus of hot water. The hot oil annulus is probably seismically transparent. Beyond that, a fast-propagating high-pressure cold oil front causes strong velocity increases by driving residual gas saturation above the bubble point. The evidence for the pressure front includes polarity reversals along the base of reservoir reflector, and wide-spread seismic changes (velocity pull-up?) below the reservoir base out to the edges of the survey. This high-pressure front could be a powerful tool for predicting future oil flow months in advance of the thermal front.

REFERENCES

Greaves, R. J., and Fulp, T. J., 1987, Three-dimensional seismic monitoring of an enhanced oil recovery process: Geophysics, **52**, no. 9, 1175–1187.

Nur, A., 1989, Four-dimensional seismology and (true) direct detection of hydrocarbons: the petrophysical basis: The Leading Edge, **8**, no. 9, 30–36.

Pullin, N. E., Jackson, R. K., Matthews, L. W., Thorburn, R. F., Hirsche, W. K., and den, B. L. D., 1987, 3-d seismic imaging of heat zones at an athabasca tar sands thermal pilot: 57th Annual Internat. Mtg., Soc. Expl. Geophys., Expanded Abstracts, Session:SEG1.7.